

Pruning the Way to Reliable Policies: A Multi-Objective Deep Q-Learning Approach to Critical Care*

Ali Shirali^{†1}, Alexander Schubert^{†1,2}, and Ahmed Alaa^{1,2}

¹University of California, Berkeley

²University of California, San Francisco

Abstract

Medical treatments often involve a sequence of decisions, each informed by previous outcomes. This process closely aligns with reinforcement learning (RL), a framework for optimizing sequential decisions to maximize cumulative rewards under unknown dynamics. While RL shows promise for creating data-driven treatment plans, its application in medical contexts is challenging due to the frequent need to use sparse rewards, primarily defined based on mortality outcomes. This sparsity can reduce the stability of offline estimates, posing a significant hurdle in fully utilizing RL for medical decision-making. We introduce a deep Q-learning approach to obtain more reliable critical care policies by integrating relevant but noisy frequently measured biomarker signals into the reward specification without compromising the optimization of the main outcome. Our method prunes the action space based on all available rewards before training a final model on the sparse main reward. This approach minimizes potential distortions of the main objective while extracting valuable information from intermediate signals to guide learning. We evaluate our method in off-policy and offline settings using simulated environments and real health records from intensive care units. Our empirical results demonstrate that our method outperforms common offline RL methods such as conservative Q-learning and batch-constrained deep Q-learning. By disentangling sparse rewards and frequently measured reward proxies through action pruning, our work represents a step towards developing reliable policies that effectively harness the wealth of available information in data-intensive critical care environments.

1 Introduction

The intensive care unit (ICU) stands out as a prime candidate for the development of data-driven decision support tools. In the ICU, a comprehensive array of physiological patient biomarkers is continuously monitored and digitally stored, offering a rich set of information to guide decisions. Patients in the ICU typically experience critical health conditions, where accurate medical decisions are crucial and can be the determinant between life and death. Moreover, decision-making in this environment is inherently sequential, with a plethora of biomarkers offering valuable, albeit noisy, insights into the patient’s evolving health status. Given these characteristics, there has been a surge of interest in exploring the prospects of reinforcement learning (RL) in critical care settings [1]–[14], where the development of personalized, data-driven treatment policies for the management of vasopressors and intravenous fluids in sepsis patients has become a key area of interest [2], [3], [8], [11], [14]–[18].

*This work has been published in the *Journal of Biomedical and Health Informatics*. 2168-2194 © 2024 IEEE. Personal use is permitted, but republication/redistribution requires IEEE permission.

Citation: A. Shirali, A. Schubert and A. Alaa, “Pruning the Way to Reliable Policies: A Multi-Objective Deep Q-Learning Approach to Critical Care,” in *IEEE Journal of Biomedical and Health Informatics*, vol. 28, no. 10, pp. 6268-6279, Oct. 2024, doi: <https://doi.org/10.1109/JBHI.2024.3415115>.

Accepted version available here: <https://ieeexplore.ieee.org/document/10559219>

[†]Equal contribution

Specifying an effective reward function is a central challenge in medical RL applications. While patient survival is a critical outcome of interest, a survival-based reward function is sparse and provides only a delayed signal, which can decrease the stability of the offline learning process. Alternatively, intermediate rewards based on medical risk scores and biomarkers provide more immediate feedback but introduce complexities (see Figure 5 for an illustrative example). These noisy representations of patient health can skew the learning process, leading to policies that may not align with optimal patient outcomes, especially if the RL model disproportionately favors optimizing intermediate rewards over nuanced, long-term objectives crucial for patient care. As a result, several studies in the medical context have focused solely on rewarding RL agents based on survival outcomes, ignoring the rich set of intermediate patient health indicators collected within the ICU environment [11], [14], [15].

To address this challenge, we propose a novel two-stage algorithm that responsibly incorporates noisy intermediate indicators into an RL framework. First, we introduce a multi-objective Q-learning algorithm that *prunes* the action set based on multiple intermediate reward signals without committing to an explicit relationship between them. Second, we learn a Q-learning policy using only the sparse main reward while constraining the action space to the pruned action set derived in the first phase. In our approach, pruning relaxes the reliance on the noisy intermediate reward indicators since we focus on removing actions that are expected to be suboptimal for any linear combination of the different reward indicators. This approach minimizes the possible distortion caused by imprecise rewards and enables the learning of more effective RL policies from sparse rewards in the second stage.

We evaluate our framework in both off-policy and offline settings using simulated environments and real data. In the off-policy setting, which includes the standard OpenAI Gym Lunar Lander environment [19] and the domain-specific Sepsis Simulator [20], our algorithm effectively prunes the action space, leading to improved policies.

In an offline setting using real health records of septic patients in the ICU, our method surpasses leading offline reinforcement learning techniques Conservative Q-Learning (CQL) [21] and Discrete batch-constrained deep Q-learning (BCQ) [22]. It excels both in terms of weighted importance sampling (WIS) estimates and in a qualitative assessment of the discriminative power of the Q-functions derived from various approaches. Additionally, our pruning step efficiently narrows the range of potential actions without excluding those often chosen by clinicians, indicating that the clinical relevance of the action set is maintained.

These results suggest that our two-stage algorithm is able to effectively incorporate information from diverse inputs while distinguishing between key outcomes and less accurate proxies. This capability is crucial in critical care settings, where intermediate indicators are plentiful and accurate responses to these signals are essential for providing decision recommendations. With this work, we aim to advance RL toward its potential to deliver personalized medical treatment policies tailored to the unique histories of individual patients.

The code to replicate our results is publicly available at the following link:

<https://github.com/alishiraliGit/multi-criteria-deep-q-learning>

2 Related Work

Multi-Objective Reinforcement Learning. Multi-objective RL methods aim to derive policies in settings with multiple reward signals. The main body of work in this area can be divided into single-policy methods and multi-policy methods. We refer the reader to Roijers, Vamplew, Whiteson, *et al.* [23] and Hayes, Rădulescu, Bargiacchi, *et al.* [24] for a survey of the field. Single-policy methods [25], [26] reduce multiple objectives into a single scalar reward, assuming a known user-specified or context-driven preference over different objectives, and then seek to maximize the scalarized objective using standard RL techniques. The major difference between various single-policy approaches lies in the way they attempt to derive preferences over objectives. These methods, however, cannot be used when the preferences themselves are unknown.

In contrast, multi-policy methods aim to estimate the Pareto frontier of a set of policies under different preferences. One way to achieve this is by training an ensemble of policies based on different reward

scalarizations [10], [27]–[30]. However, these methods require exhaustive training and, in some cases, non-trivial scalarizations. Another approach is a value-based method, which extends the standard scalar variables in RL algorithms to vector variables and uses updating rules in the vector space. Early work in this direction explored the problem of acquiring all Pareto optimal policies simultaneously [31]–[33]. These methods focused on applications in online settings and on small, finite-state spaces. Lizotte and Laber [34] extended Barrett and Narayanan [31]’s framework to real-valued state features but with exponential complexity in the time horizon and the size of the action space. A variation of this line of work focuses on the development of non-deterministic policies (or set-valued policies) [35], [36], which provide a set of potential solutions instead of a single action.

In this work, we build on the value-based approach to derive a pruning function using an approximate problem formulation that runs for arbitrarily long trajectories. Different from prior studies that focus on directly inferring Pareto-optimal policies, we utilize multi-objective RL to prune the action space by identifying and eliminating inferior state-action pairs. This allows us to reduce the complexity of the learning problem in the second phase of our algorithm where we train using a sparse reward alone. To our knowledge, this is one of the earliest efforts in this direction.

Reinforcement Learning in Health. Recent literature in healthcare has extensively explored RL, particularly for developing personalized treatment plans for sepsis patients in ICU settings [1], [2], [8], [9], [11], [14]–[18], [37]–[40]. Many studies rely on sparse rewards [11], [14], [15], with some using the intermediate SOFA score as the sole reward metric [16], which may introduce bias in specific populations [41]. Others have explored inverse RL to deduce reward functions from historical data [18].

In addition to the direct learning of treatment policies, another line of work has focused on detecting medical dead-end states [3], [42]–[44]. For instance, Fatemi, Killian, Subramanian, *et al.* [3] developed an RL algorithm to identify and avoid states from which no action can achieve a positive terminal outcome (e.g., survival). While the aim of this method is conceptually close to the goal of our pruning stage, we propose a distinct technical approach to achieve this goal. Fatemi, Killian, Subramanian, *et al.* [3]’s work focuses on classifying states that should be avoided; in contrast, our method directly identifies and excludes dominated *state-action pairs*. Furthermore, our method does not stop at identifying risky actions but leverages the pruned action space for subsequent training of an optimal policy.

3 Notation and Preliminaries

Reinforcement Learning. Following the terminology commonly adopted in RL, consider an *agent* interacting with an *environment*. As the agent executes an *action*, denoted as $a \in \mathcal{A}$, in a given *state*, denoted as $s \in \mathcal{S}$, a *reward*, expressed as $r(s, a)$, materializes, and the environment’s state subsequently updates to s' . The agent can then utilize this reward as feedback to make better future action choices. The agent’s decision-making process is described by a *policy*. In general, a policy $\pi : \mathcal{S} \rightarrow \Delta(\mathcal{A})$ provides a distribution over potential actions for each state. A deterministic policy $\pi : \mathcal{S} \rightarrow \mathcal{A}$ singles out a specific action given the current state. Our study particularly focuses on *offline* RL, where the aim is to devise an effective policy based on previously collected data. Additionally, our algorithms are also applicable in *off-policy* settings, where the agent interacts with the environment at selected time steps. We denote the available data as a set of transitions \mathcal{D} . Each transition is a tuple (s, a, s', r) , representing that action a taken at state s results in a transition to state s' and a reward of r .

Q-Learning. A standard (scalar) *Q-function* $Q^\pi : \mathcal{S} \times \mathcal{A} \rightarrow \mathbb{R}$ estimates the value of policy π at state s given that the agent takes action a at s and follows policy π thereafter. This value represents the expected discounted sum of rewards, where rewards obtained at later timesteps are discounted by a factor of γ . If the Q-function is implemented via a deep neural network it is occasionally referred to as a *Q-network*. Throughout this work, we use the terms Q-function and Q-network interchangeably. In the context of Q-Learning, we sample a batch of transitions \mathcal{B} from \mathcal{D} and employ the Bellman equation to update the

Q-network, assuming the *optimal action* will be taken at subsequent steps:

$$Q(s, a) \leftarrow r + \gamma \max_{a'} Q(s', a'). \quad (1)$$

Let the Q-network be parameterized by θ . Then the above notation is a shorthand to update θ from its current value θ_0 by minimizing the loss

$$\mathcal{L}(\theta) = \sum_{(s,a,s',r) \in \mathcal{B}} (Q_\theta(s, a) - r - \gamma \max_{a'} Q_{\theta_0}(s', a'))^2.$$

This update is typically implemented via a single or a couple of gradient descent steps. However, Q-learning based on the above formulation suffers from a fast-moving target and overestimation. These challenges can be addressed by employing a target network Q' along with an update rule, recognized as double Q-learning [45]:

$$Q(s, a) \leftarrow r + \gamma Q'(s', \arg \max_{a'} Q(s', a')).$$

In double Q-learning, Q' is updated by $Q' \leftarrow Q$ after hundreds or thousands of updates to Q . The final deterministic policy can then be extracted as $\pi(s; Q) = \arg \max_a Q(s, a)$.

Q-Learning With Softmax Policies In the original Bellman update, the optimal policy is deterministic, selecting the action that maximizes the Q-function for each state. However, empirical evidence has shown that applying a softmax operator tends to yield superior policies, particularly in the context of deep Q-networks. This relaxation has also garnered recent theoretical support [46]. Formally, given a Q-function Q , we can derive a stochastic softmax policy π^β as

$$\pi^\beta(a|s; Q) = \frac{\exp(\beta Q(s, a))}{\sum_{\bar{a}} \exp(\beta Q(s, \bar{a}))},$$

where β is an inverse temperature parameter. Note that in the limit of $\beta \rightarrow \infty$, the softmax policy converges to a deterministic argmax policy. Let us define

$$\text{softmax}_{a'} Q(s', a') := \sum_{a'} \pi^\beta(a'|s'; Q) \cdot Q(s', a').$$

We dropped the dependence on π^β from the softmax notation for brevity. Note that $\text{softmax}_{a'} Q(s', a') \rightarrow \max_{a'} Q(s', a')$ as $\beta \rightarrow \infty$. A Bellman update using softmax can then be obtained by substituting the max with a softmax operator in Equation 1. Similarly, we can derive double Q-learning using a softmax policy as

$$Q(s, a) \leftarrow r + \gamma \sum_{a'} \pi^\beta(a'|s'; Q) \cdot Q'(s', a').$$

Vector-Valued Reward and Q-Function. In many practical scenarios, reward signals can be multi-dimensional. In particular, consider a scenario with a sparse main reward r_* and a set of d noisy but more frequent auxiliary rewards. In these cases, we gather all the rewards into a *vector reward* $\mathbf{r} \in \mathbb{R}^d$ and use r_i to refer to the i^{th} reward. We introduce a *vector-valued Q-function* $\mathbf{Q} : \mathcal{S} \times \mathcal{A} \rightarrow \mathbb{R}^d$ that outputs a vector of estimated Q-values for any state-action pair. The i^{th} dimension of \mathbf{Q} , denoted by Q_i , corresponds to the Q-value associated with reward r_i . We discuss learning vector-valued Q-functions in Section 4.1.

4 Methods

Our study aims to develop a method that effectively incorporates frequent but noisy auxiliary rewards without diverting the policy from maximizing the primary sparse reward of interest. We hypothesize

that while some biomarkers or clinical risk scores might be too noisy or imprecise to be directly used in deriving an optimal policy, they may still be useful to *identify actions to avoid*. Hence, we propose a two-stage algorithm: In the first phase, we learn a vector-valued Q-function relying on all rewards. This Q-function will subsequently be used to *prune* the action set at each state. Then in the second phase, we search for the optimal policy based on the (accurate) sparse reward. Actions dropped in the first phase won't be available to the policy of the second phase, which reduces the complexity of the learning problem and thus facilitates learning from the sparse reward. Figure 1 illustrates our method.

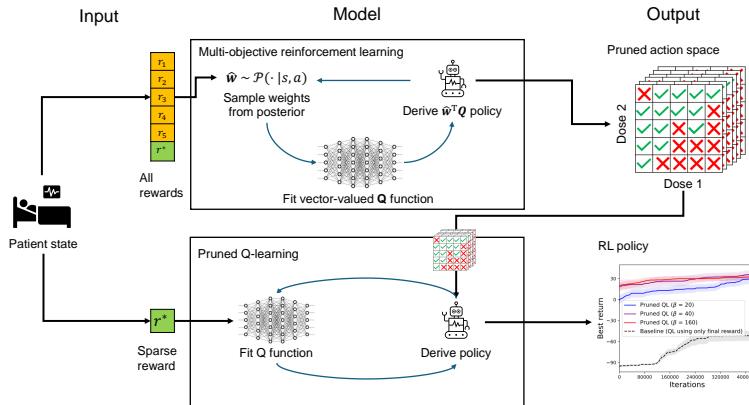


Figure 1: Illustration of our algorithm. The model first leverages all rewards in order to prune the action space for each state. Then another policy is trained based on the sparse main reward but with its action space restricted to the actions available after pruning in the first stage.

4.1 Phase 1: Multi-Objective Deep Q-Learning

The first step of our algorithm aims to generate a pruned list of permissible actions for each state. We achieve this by leveraging several intermediate reward signals, where we use a vector-valued Q-learning method to learn optimal policies across various reward weightings. For the offline setting, we further borrow ideas from conservative Q-learning to ensure that the recommendation of the learned policy stays close to the state-action pairs observed in the dataset. The following outlines the technical implementation.

A Vector-Valued Q-Learning Approach. To derive a pruning policy we first need to learn a Q-function that enables us to estimate policy returns for different state-action pairs. A direct method to combine a sparse main reward and intermediate reward signals is through scalarization of the reward vector \mathbf{r} . In its simplest form, consider a linearly weighted combination $\mathbf{w}^\top \mathbf{r}$ where $\mathbf{w} \in \mathcal{W} \subseteq \mathbb{R}^d$ determines the relative importance of each reward component. We assume $w_i \geq 0$ and $\sum_{i=1}^d w_i = 1$. By using the combined reward as the standard Q-learning objective, we can obtain the Q-function $Q^{\mathbf{w}}$ and its corresponding (possibly stochastic) policy $\pi^\beta(\cdot | \cdot; Q^{\mathbf{w}})$. However, the best \mathbf{w} may not be known a priori. To address this, we propose learning a vector-valued Q-function such that $Q^{\mathbf{w}}(s, a) \approx \mathbf{w}^\top \mathbf{Q}(s, a)$ for almost every $\mathbf{w} \in \mathcal{W}$. This approach avoids the need to explicitly scalarize the intermediate rewards or train a computationally expensive ensemble of models with different reward weightings.

Such a Q-function cannot be learned based on a naive extension of the Bellman update. To observe this consider a fixed \mathbf{w} and plug $Q^{\mathbf{w}}(s, a) = \mathbf{w}^\top \mathbf{Q}(s, a)$ into the Bellman update of $Q^{\mathbf{w}}$:

$$\mathbf{w}^\top \mathbf{Q}(s, a) \leftarrow \mathbf{w}^\top \mathbf{r} + \gamma \operatorname{softmax}_{a'} \mathbf{w}^\top \mathbf{Q}(s', a'). \quad (2)$$

The above update depends on \mathbf{w} and, generally, cannot hold true for all $\mathbf{w} \in \mathcal{W}$: The left-hand side of the update equation is linear in \mathbf{w} , but the right-hand side, involving a softmax operation, introduces non-linearity.¹

To ensure the update equation is universally applicable for any \mathbf{w} , we approximate the softmax with a linear conservative estimate as

$$\text{softmax}_{a'} \mathbf{w}^\top \mathbf{Q}(s', a') \approx \sum_{a'} \pi^\beta(a'|s'; \hat{\mathbf{w}}^\top \mathbf{Q}) \cdot \mathbf{w}^\top \mathbf{Q}(s', a'), \quad (3)$$

where $\hat{\mathbf{w}}$ is sampled from a prior distribution \mathcal{P} . To see that this approximation is conservative, consider large values of β . In this case, π^β converges to an argmax policy, so the left-hand side of Equation 3 converges to $\max_{a'} \mathbf{w}^\top \mathbf{Q}(s', a')$ while the right-hand side of Equation 3 converges to

$$\mathbf{w}^\top \mathbf{Q}(s', \arg \max_{a'} \hat{\mathbf{w}}^\top \mathbf{Q}(s', a')),$$

serving as a lower bound for the left-hand side.

Using the approximation in Equation 3, both sides of Equation 2 become linear in \mathbf{w} and we can thus derive a vector update for \mathbf{Q} that is independent of \mathbf{w} :

$$\mathbf{Q}(s, a) \leftarrow \mathbf{r} + \gamma \sum_{a'} \pi^\beta(a'|s'; \hat{\mathbf{w}}^\top \mathbf{Q}) \cdot \mathbf{Q}(s', a').$$

Posterior Sampling of Reward Weights. The approximation in Equation 3 may be loose for a specific but unknown reward weighting \mathbf{w} , particularly when the optimal actions for \mathbf{w} and $\hat{\mathbf{w}}$ differ substantially. A domain-knowledge-informed prior distribution \mathcal{P} over the space of possible weightings \mathcal{W} can partially mitigate this issue by ruling out implausible weightings. We then note that for a given \mathbf{w} , if the probability $\pi^\beta(a|s; \mathbf{w}^\top \mathbf{Q})$ is very low, the approximation’s accuracy is less critical as it underestimates the value of an action that is unlikely to be chosen. In contrast, a high probability $\pi^\beta(a|s; \mathbf{w}^\top \mathbf{Q})$ indicates the need for a precise approximation. This observation can be formalized by obtaining a posterior

$$\mathcal{P}(\mathbf{w}|s, a) \propto \mathcal{P}(\mathbf{w}) \cdot \pi^\beta(a|s; \mathbf{w}^\top \mathbf{Q}),$$

and drawing $\hat{\mathbf{w}}$ from the posterior. Intuitively, the prior is upscaled over a \mathbf{w} that suggests action a is likely to be chosen at s , resulting in a tighter approximation of Equation 3 for such weightings. Any posterior sampling method can be used to draw $\hat{\mathbf{w}}$. For simplicity, we use a single iteration of particle filtering, which involves sampling particles from \mathcal{P} , reweighting them according to π^β , normalizing the weights, and then resampling.

To further improve the stability and performance of the algorithm, we also use double Q-learning [45] by introducing another vector-valued Q-network \mathbf{Q}' as the target network. The target network \mathbf{Q}' is updated after multiple updates of \mathbf{Q} by copying the weights from \mathbf{Q} . Our update rule for \mathbf{Q} is

$$\mathbf{Q}(s, a) \leftarrow \mathbf{r} + \gamma \sum_{a'} \pi^\beta(a'|s'; \hat{\mathbf{w}}^\top \mathbf{Q}) \cdot \mathbf{Q}'(s', a'), \quad (4)$$

where we draw $\hat{\mathbf{w}}$ from posterior $\mathcal{P}(\cdot|s, a)$. We will refer to this method as *multi-objective Q-learning (MQL)* in the following sections.

Adaptation to Offline Learning. Q-learning is prone to overestimating Q-values for states and actions not present in the dataset. To overcome this challenge we borrow ideas from conservative Q-learning (CQL) [21] by including an additional term in the Q-learning loss function that penalizes out-of-distribution (s, a) pairs. Specifically, for a Q-function \mathbf{Q} parameterized by θ , we calculate the loss function

$$\mathcal{L}_\alpha(\theta; (s, a, s', \mathbf{r})) = \mathcal{L}(\theta; (s, a, s', \mathbf{r})) + \frac{\alpha}{d} \sum_{i \in [d]} \left[\log \left(\sum_{\bar{a} \in \mathcal{A}} \exp Q_{i, \theta}(s, \bar{a}) \right) - Q_{i, \theta}(s, a) \right].$$

¹This statement also holds for deterministic policies, where the right-hand side would be piecewise linear.

Here, $\mathcal{L}(\theta; (s, a, s', \mathbf{r}))$ is a standard Q-learning loss based on the update rule described in Equation 4, and i indexes over d reward dimensions. We will refer to this method as *multi-objective conservative Q-learning (MCQL)*.

Pruning the Action Space. Using the vector-valued Q-function \mathbf{Q} obtained from the MCQL or MQL method, we can now prune the action space. First, for a given \mathbf{Q} and a prior \mathcal{P} over reward weightings, define a stochastic policy $\pi_{\mathcal{P}}^{\beta}(a|s)$ as

$$\pi_{\mathcal{P}}^{\beta}(a|s) := \mathbb{E}_{\mathbf{w} \sim \mathcal{P}}[\pi^{\beta}(a|s; \mathbf{w}^{\top} \mathbf{Q})].$$

We then propose a pruning function $\Pi^{\beta} : \mathcal{S} \rightarrow 2^{\mathcal{A}}$ by sampling from $\pi_{\mathcal{P}}^{\beta}$ as follows:²

1. At state s , draw m actions $a^{(k)} \sim \pi_{\mathcal{P}}^{\beta}(\cdot|s)$ for $k \in [m]$:
 - (a) Draw m samples $\mathbf{w}^{(k)} \sim \mathcal{P}$ for $k \in [m]$.
 - (b) For each $\mathbf{w}^{(k)}$, draw $a^{(k)} \sim \pi^{\beta}(\cdot|s; \mathbf{w}^{(k)\top} \mathbf{Q})$.
2. Set $\Pi^{\beta}(s) = \{a^{(k)} \mid k \in [m]\}$.

The choice of m and β determines the expected size of the set $\Pi^{\beta}(s)$. As a rule of thumb, actions with $\pi_{\mathcal{P}}^{\beta}(a|s) < \frac{1}{m}$ are unlikely to remain in the action set after pruning. In practice, we set m to be at least three times the size of the action space $|\mathcal{A}|$, ensuring that all actions have a chance to appear in Π^{β} while still allowing rare actions to be pruned. Adjusting β then controls the pruning strictness, with higher values leading to more deterministic policy selections. We treat β as a hyperparameter.

4.2 Phase 2: Q-Learning with Pruning

After obtaining a pruned action space, we employ double Q-learning with the main reward and limit actions to those selected by the pruning function Π^{β} :

$$Q(s, a) \leftarrow r + \gamma Q'(s', \arg \max_{a' \in \Pi^{\beta}(s')} Q(s', a')). \quad (5)$$

By using a loss function similar to conservative Q-learning [21], we can also obtain a pruned conservative Q-learning approach.

Examining Equation 5, we observe that $\Pi^{\beta}(s')$ is the only place where we incorporate noisy intermediate rewards in the final policy. Optimization of the Q-function is thus solely guided by the main reward, ensuring that our learned policy remains focused on our original goal. We believe that the disentanglement of noisy and accurate rewards through this two-stage algorithm enables us to effectively incorporate information from intermediate signals to simplify the learning problem while minimally influencing the policy’s primary objective.

In summary, our method termed *Pruned QL* combines MQL for pruning and Q-learning for final action selection. In offline contexts, *Pruned CQL* integrates MCQL and CQL.

5 Off-Policy Experiments

We begin by evaluating our method in an off-policy setting using two environments: A variation of the OpenAI Gym Lunar Lander [19] and the medical domain-specific Sepsis Simulator [20]. These simulated environments allow us to directly observe the performance of the learned policy when rolled out.

Both environments are well-suited for testing our method’s capabilities. In Lunar Lander, the objective is to land a small spaceship on the moon successfully. In addition to the main objective, three intermediate

²An alternative approach to prune the action set could be to drop actions with $\pi_{\mathcal{P}}^{\beta}(a|s)$ below a threshold. However, calculating $\pi_{\mathcal{P}}^{\beta}(a|s)$ requires a posterior calculation that can be computationally difficult.

rewards related to the lander’s shape and fuel efficiency guide the landing process. Besides the main objective, there are three intermediate rewards related to the lander’s shape and fuel efficiency that guide the landing process. The combination of a sparse main objective and informative intermediate signals makes Lunar Lander an ideal choice for evaluating our approach. The evaluation results presented for this environment reflect a setting where rewards are solely based on the successful completion of the primary objective: +100 for a successful landing and −100 for failure.

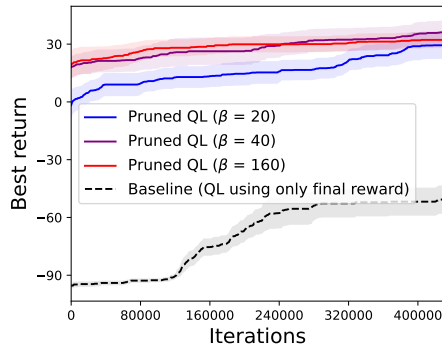
The Sepsis Simulator [20] models the simplified physiology of patients with sepsis. The actor chooses between three binary treatments: antibiotics, vasopressors, and mechanical ventilation. Each treatment can affect vital signs such as heart rate, blood pressure, oxygen concentration, and glucose levels, altering their values with predefined probabilities. Patients are discharged when all vital signs normalize and treatments cease; death occurs if three or more vitals become abnormal. Intermediate reward signals are derived from the vital sign values, while the main objective is represented by a sparse reward: +100 for patient discharge and -100 for patient death. To increase the complexity and mimic the challenge of observing final patient outcomes in real health records, we omit the final reward for a random set of 90% of the trajectories. Additionally, we limit the episode length to a maximum of 20 steps.

Figure 2 presents the main off-policy evaluation results. We conduct two experiments for each environment. First, to analyze the performance of our method compared to a policy that only has access to the sparse reward signal, Figure 2(a) and 2(b) display the best return achieved during training for the Pruned QL algorithm under different pruning strengths, compared to a Q-learning policy trained using only sparse reward information. Our observations indicate that our method consistently outperforms the sparse reward policy across different pruning strengths in both the Lunar Lander and Sepsis Simulator environments. Notably, the Pruned QL method achieves high returns after fewer iterations and leads to policies that attain higher returns after the full 500,000 training iterations. These results demonstrate that simple Q-learning solely based on the sparse reward can be slow and ineffective in both settings. In contrast, PrunedQL effectively leverages the intermediate reward signals to derive a pruned action space using which it is possible to achieve effective learning performance from a sparse reward.

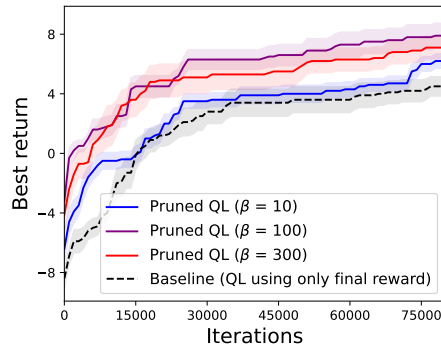
We next demonstrate that Pruned QL also performs better than standard Q-learning methods when incorporating intermediate rewards during the learning process. Figure 2(c) and 2(d) plot the performance of different Pruned QL and Q-learning policies with varying strengths of intermediate reward weights. For Pruned QL, reward weights are the concentration parameters of the prior Dirichlet distribution, with higher weights indicating that intermediate rewards are more important compared to the sparse reward. By including intermediate reward data, the baseline Q-learning models now have access to the same information as the Pruned QL models.

Our results indicate that incorporating intermediate rewards does not inherently enhance model performance. Although the baseline model achieves results comparable to the Pruned QL policy when equipped with the correct (albeit typically unknown) weightings, alterations in these weightings can cause significant performance degradation. For example, in the Sepsis Simulator environment, increasing the intermediate reward weight from 0.1 to 1 causes the model return to decline from 2 to −8, performing worse than a model trained with sparse rewards alone. In many real-world scenarios where the true reward weights are unknown, this might discourage the inclusion of intermediate reward information during model development. In contrast, the Pruned QL method demonstrates stable performance across various reward-weighting priors, effectively utilizing intermediate reward information. We further find that our method shows strong robustness to noise in the intermediate reward signals as outlined in Section B.

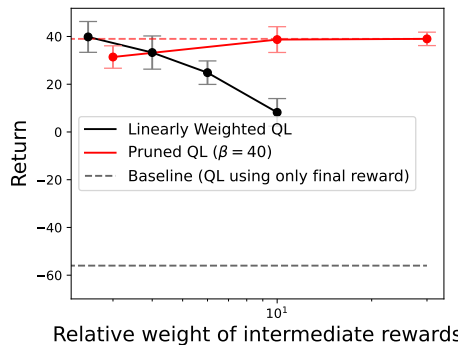
Model Parameters. We employ a Dirichlet distribution as the prior for reward weighting, with a concentration parameter of 1 for the main reward and 10 for intermediate rewards. We choose a Dirichlet distribution due to its flexibility, intuitiveness, and common usage for modeling non-negative variables that sum to one, such as probabilities. As shown in Figure 2(d), our results are not sensitive to this parameter choice. We set the discount factor $\gamma = 1$, not discounting future rewards. The Q-function is implemented as a 3-layer feed-forward neural network with ReLU activation, and we use the Adam optimizer with a learning rate of 10^{-4} . For Lunar Lander, the target network is updated once every 3000 updates of the Q-network, while for the Sepsis Simulator, it is updated every 10000. For the remaining Q-learning parameters, please refer to the accompanying code.



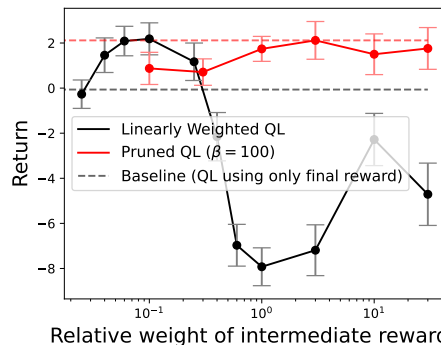
(a) Lunar Lander: Best return during training



(b) Sepsis Simulator: Best return during training



(c) Lunar Lander: Policy return under different intermediate reward weightings ($\beta = 40$)



(d) Sepsis Simulator: Policy return under different intermediate reward weightings ($\beta = 100$)

Figure 2: Performance of Pruned QL in the Lunar Lander and Sepsis Simulator environments. (a) and (b) demonstrate that Pruned QL consistently achieves higher returns compared to a baseline Q-learning method that only has access to the sparse reward. Returns are estimated on new rollouts, not in the training data. (c) and (d) highlight that Pruned QL matches oracle Q-learning across varying intermediate reward weights, demonstrating its robustness and ability to leverage reward information effectively.

6 Offline Experiments

6.1 Cohort and Study Design

We evaluate our framework in a real-life offline learning setting by training and evaluating policies for the management of vasopressor and intravenous (IV) fluids in septic patients at intensive care units (ICU). Existing works [3], [11], [15] in this area have mainly focused on reward specifications based on 90-day mortality. In contrast, we investigate whether Pruned CQL can facilitate learning superior policies by incorporating information from intermediate severity proxies such as the SOFA score [47] and the patient’s lactate level.

Data. We use data from a cohort of septic ICU patients in the MIMIC (Medical Information Mart for Intensive Care)-III dataset (v1.4) [48]. This dataset consists of deidentified electronic health records of over 40,000 patients who were admitted to the critical care units of the Beth Israel Deaconess Medical Center in Boston between 2001 and 2012. To construct our sample, we followed the preprocessing steps applied in Komorowski, Celi, Badawi, *et al.* [11]. We excluded patients younger than 18 years old at ICU admission or where mortality and intravenous fluid intake have not been documented. A trajectory

includes data from 24 hours before the sepsis onset up until 48 hours after the onset, recorded in 4-hour intervals. For every trajectory, we extracted a set of 48 variables, including demographics, Elixhauser comorbidity index [49], vital signs, laboratory test results, and medication dosing decisions. All models are trained on 80% of the data, validated on 5%, and tested on 15% for the final evaluation.

Action Set and State Space. Following previous works [3], [11], we discretize actions into 25 treatment choices (5 discrete levels for IV fluids and 5 discrete levels for vasopressor dosage). To derive the state space, we applied K-means clustering to the 48-dimensional features and obtained 752 clusters. As the resulting cluster indicators were not numerically meaningful, we additionally applied the continuous bag of words method [50] to the patients’ state trajectories. This provided us with a 13-dimensional representation for each cluster. Thus, our problem formulation is based on a 25-dimensional action space and 752 states, where each state is represented by a 13-dimensional vector. The resulting dataset consists of 20,912 ICU stay trajectories, of which 4,917 resulted in patient death within 90 days of the patient’s critical care visit.

Reward Specification. We assign a reward of +100 to the final state of a trajectory if the patient survives for at least 90 days past ICU admission, and a reward of −100 otherwise. Achieving a low 90-day mortality is the ultimate goal of our learning agent but since this is a sparse and delayed signal, we further include four medically-motivated rewards that are observed more frequently throughout the patient’s stay:

- **One-period SOFA score change:** The negative of the one-period change in SOFA score.
- **Two-period SOFA score change:** The negative of the two-period change in SOFA score.
- **One-period lactate level change:** The negative of the one-period change in the lactate level.
- **Two-period lactate level change:** The negative of the two-period change in the lactate level.

SOFA [47] is a medical risk score that summarizes the extent of a patient’s organ failure and in recent years has become a key indicator of the sepsis syndrome [51]. Arterial lactate levels are an important biomarker for septic shock because they are closely associated with cellular hypoxia. Sepsis can cause an imbalance in oxygen supply and demand, resulting in inadequate delivery of oxygen to the cells and tissues. This can lead to anaerobic metabolism and the production of lactate as a byproduct. Increased arterial lactate levels, therefore, indicate that there is a mismatch between oxygen supply and demand and that the body is experiencing hypoxia [52].

Model Parameters. The model hyperparameters in the offline setting are largely analogous to those in the off-policy setting. Additionally, we select a CQL-alpha parameter of 0.001. The target Q network is updated every 1000 training steps during the first phase and every 8000 steps during the second phase. For further implementation details, please refer to the code repository associated with this paper.

6.2 Policy Evaluation Approach

In the offline RL setting, rolling out the learned policies to observe their returns is not feasible. Therefore, we evaluate the policies using weighted importance sampling (WIS) and a descriptive measure to assess the Q-functions’ ability to distinguish between high and low mortality trajectories.

Various methods exist for estimating policy values in offline settings, each with limitations. For an empirical comparison of different methods, see Tang and Wiens [53], and for practical considerations, see Gottesman, Johansson, Meier, *et al.* [54].

Importance sampling methods are an effective class of techniques for policy evaluation in the offline setting. The main idea behind these evaluation approaches is to re-weight trajectories based on their likelihood of occurrence to estimate the policy value. This requires a stochastic policy and knowledge of the behavioral policy. To accommodate our deterministic policy in phase 2, we follow Tang, Modi,

Sjoding, *et al.* [40] by *softening* our policy: $\tilde{\pi}(a|s) = (1 - \epsilon)\mathbb{1}\{a = \pi(s)\} + \frac{\epsilon}{|\mathcal{A}|-1}\mathbb{1}\{a \neq \pi(s)\}$, where ϵ is set to 0.01. To calculate the importance ratio, we approximate the physician’s policy with a stochastic policy using a multi-class logistic regression with cross-entropy loss. We train this classifier to predict the next action based on the 13-dimensional state space. We then implement WIS to estimate policy values due to its lower variance compared to ordinary importance sampling.

One drawback of the WIS estimator is its potential bias. This bias arises because the estimator conservatively relies on the observed data generated by the behavior policy, which may not adequately represent the target policy’s distribution. Additionally, normalizing or clipping the importance weights to control variance further introduces bias, skewing the estimates towards trajectories that are more common under the behavior policy.

To supplement the WIS evaluation, we propose a descriptive measure that evaluates our Q-function’s ability to differentiate between patient survival and death trajectories. This is relevant since a high capacity of a Q-function to distinguish between low and high-risk state-action pairs increases our confidence that choosing the actions with the highest predicted Q-value is beneficial. We adopt the following approach to construct such a descriptive measure. Consider a trajectory τ from the test data and let r_*^τ be the mortality-based reward assigned to its final state. We compute $Q(s, a)$ for each state-action pair $(s, a) \in \tau$. Note that $Q(s, a)$ is supposed to be the expected return from the optimal policy at state s followed by action a and not the return of the physician’s policy r_*^τ . But if the optimal policy is sufficiently similar to the physicians, $Q(s, a)$ shall reflect r_*^τ , and we would like to see a larger $Q(s, a)$ if τ results in the patient survival. To measure this association, we bin the Q-values into quartiles and calculate the mortality rate in the lower quartile range $MR(Q_1)$ and the mortality rate in the upper quartile range $MR(Q_3)$. We then report the difference $\Delta MR = MR(Q_1) - MR(Q_3)$. A larger ΔMR indicates that the policy is more effective in distinguishing survival from death trajectories.

6.3 Offline Evaluation Results

We evaluate Pruned CQL against standard conservative Q-learning (CQL) [21] and discrete batch-constrained Q-learning (BCQ) [22]. Discrete BCQ also uses a threshold rule to constrain the action space of its policy, allowing only actions whose probability relative to the most likely action under the behavior policy exceeds a certain threshold t . However, it focuses on enforcing similarity to the behavior policy rather than leveraging intermediate reward signals as our method. Additionally, Discrete BCQ relies on an explicit estimation of the behavior policy.

Table 1 summarizes the offline evaluation results, demonstrating Pruned CQL’s superior performance in terms of both ΔMR and WIS. The Pruned CQL policy with $\beta = 160$ achieves a WIS of 66, surpassing the behavior policy (WIS of 51) and nearly doubling the best CQL policy’s performance (WIS of 35). Additionally, Pruned CQL consistently outperforms Discrete BCQ in both WIS and ΔMR . Discrete BCQ’s ΔMR is about 10 percentage points lower than CQL or Pruned CQL, suggesting a potentially inflated WIS value due to its similarity with the behavior policy. Additional findings in appendix Section C.1 illustrate that stratifying trajectories based on the Q-values predicted by Pruned CQL allows to effectively distinguish between death and survival trajectories.

Table 1 demonstrates that stricter pruning leads to policies that closely align with physician behavior. This alignment is likely driven by the pruning step enforcing greater consideration of key intermediate severity indicators crucial for physician decision-making. Similarly, higher conservativity α in Baseline CQL also yields greater agreement. Figure 3 illustrates this relationship for varying CQL- α and pruning strength β . We generally observe that increasing these hyperparameters enhances performance in terms of WIS, while maintaining or reducing performance in ΔMR , likely due to WIS’s bias towards the behavior policy. Furthermore, Pruned CQL consistently outperforms baseline CQL in both ΔMR and WIS-value at similar agreement levels. These findings suggest that our pruning approach is an effective alternative to the standard CQL loss, to increase safety by closely aligning the learned RL policy with physician practices.

Table 1: Comparison of different methods in terms of ΔMR , WIS-based policy value, and the share of common actions between the learned and the behavioral policy. Standard errors are calculated based on ten random seeds. Best result per column is underlined. The behavior policy has a return of 51.9.

Model	ΔMR (%)	Value (WIS)	Behavior policy overlap (%)
CQL($\alpha = 0.001$)	24.6 ± 1.0	14 ± 18	10.4 ± 0.7
CQL($\alpha = 0.005$)	23.6 ± 1.0	35 ± 21	18.6 ± 0.6
CQL($\alpha = 0.01$)	22.6 ± 0.9	26 ± 25	26.2 ± 1.0
<hr/>			
Discrete BCQ ($t = 0.05$)	12.9 ± 0.8	31 ± 26	36.5 ± 0.3
Discrete BCQ ($t = 0.1$)	13.8 ± 0.7	47 ± 24	39.6 ± 0.4
Discrete BCQ ($t = 0.3$)	14.8 ± 1.1	51 ± 22	<u>42.8 ± 0.3</u>
<hr/>			
Pruned CQL($\alpha = 0.001, \beta = 20$)	24.5 ± 0.9	32 ± 12	11.3 ± 1.2
Pruned CQL($\alpha = 0.001, \beta = 40$)	<u>25.2 ± 0.6</u>	41 ± 15	15.6 ± 0.9
Pruned CQL($\alpha = 0.001, \beta = 160$)	24.2 ± 1.1	<u>66 ± 19</u>	22.1 ± 0.9

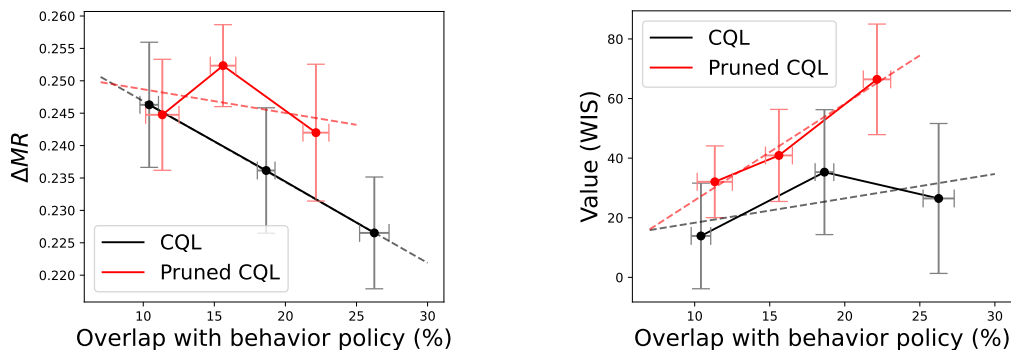


Figure 3: Comparison of Pruned CQL and CQL in terms of ΔMR and WIS-based policy value, for different degrees of overlap with the behavior policy. Dashed lines display linear fits.

6.4 Pruning Analysis

To evaluate the quality of our pruning method, we address two key questions: 1) Does our pruning procedure in phase 1 significantly reduce the size of the action space? 2) Is the resulting action space consistent with current medical practice?

Table 2 presents the average number of available actions after pruning and the corresponding recall of these action sets. Since there is no ground truth for the best policy, we define recall based on whether the pruned action sets contain the actions taken by physicians in each respective state in the test set. Given that physicians are highly trained professionals and may have access to additional indicators not captured in our records, our goal is to retain their decisions among the available options as much as possible. Our results indicate that the pruning procedure significantly reduces the size of the original

Table 2: Mean action set size and recall for different pruning levels. The initial action set size was 25.

β	Num. of available actions after pruning	Recall (%)
20	19.7 ± 0.3	94.7 ± 0.3
40	11.6 ± 0.7	83.3 ± 1.4
160	4.1 ± 0.3	49.4 ± 1.9

25-dimensional action space: Moderate pruning with $\beta = 40$ reduces the mean action set size to less than half, while stricter pruning with $\beta = 160$ reduces the average number of available actions to nearly one-sixth. Despite such aggressive pruning, our method maintains a high recall, ranging from 49% to over 94%, well beyond the chance level.

To further investigate the pruning behavior, Figure 4 shows the distribution of removed actions compared to the actions taken by physicians in the test set for a pruning strength of $\beta = 40$. Similar patterns are observed for both less stringent and more stringent pruning levels, as detailed in Figure 8. The figure indicates that our procedure primarily prunes extreme dosing regimes or incoherent decisions, such as administering a low intravenous fluid dose while simultaneously assigning a high vasopressor dose. These findings support the notion that the pruning procedure reduces the complexity of the reinforcement learning problem while retaining relevant actions for the subsequent learning stage.

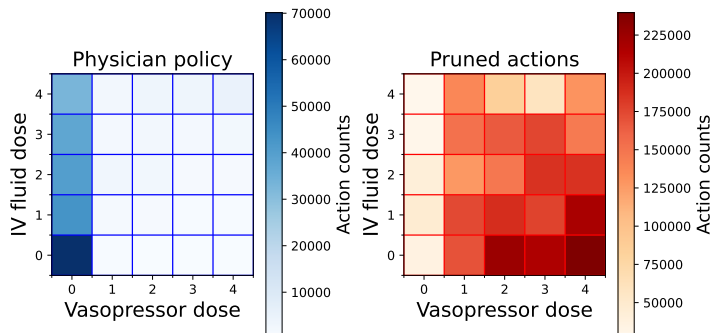


Figure 4: Distribution of physician’s actions and pruned actions ($\beta=40$).

7 Conclusion and Discussion

In this study, we introduced a novel RL method that utilizes action space pruning to facilitate learning when the main reward signal is sparse, intermediate signals are approximate, and there is ambiguity about the optimal reward component weights. Our algorithms effectively integrate more frequent but imprecise reward proxies into learning.

We demonstrated the effectiveness of our approach in off-policy settings using the Lunar Lander and Sepsis Simulator environments, where action-space pruning enables Q-learning from sparse rewards alone, outperforming standard Q-learning approaches. Furthermore, in an offline setting prescribing vasopressor and intravenous fluid dosing for septic ICU patients, our method learned more effective policies compared to leading offline RL methods, including Conservative Q-learning and Discrete BCQ. Our learning framework efficiently incorporates recurrent yet imprecise reward signals while preventing such signals from causing the policy to diverge from maximizing the primary reward of interest. Although motivated by healthcare applications, our approach is applicable to other domains where the true reward signal is sparse and available proxies are frequent but imperfect indicators of the outcome of interest.

Limitations. First, our results are based on data up to 2012, and sepsis treatment guidelines have evolved since then, meaning the estimated physician policies may reflect a slightly outdated standard of care. Second, our method relies on the availability of meaningful intermediate reward signals that can serve as proxies for the final outcome of interest, and it may not be applicable in cases where such signals are not available. Finally, we utilized weighted importance sampling (WIS) for offline evaluation. Although WIS is a widely accepted technique for evaluating RL policies in offline settings, it is also known to have high variance and is dependent on accurate estimation of the behavior policy [53]. We partially addressed this issue by evaluating our policy using a related descriptive measure that highlights consistent results with the provided WIS estimates.

References

- [1] K. E. Henry, D. N. Hager, P. J. Pronovost, and S. Saria, “A targeted real-time early warning score (trewscore) for septic shock,” *Science translational medicine*, vol. 7, no. 299, 299ra122–299ra122, 2015.
- [2] T. Nanayakkara, G. Clermont, C. J. Langmead, and D. Swigon, “Unifying cardiovascular modelling with deep reinforcement learning for uncertainty aware control of sepsis treatment,” *PLOS Digital Health*, vol. 1, no. 2, e0000012, 2022.
- [3] M. Fatemi, T. W. Killian, J. Subramanian, and M. Ghassemi, “Medical dead-ends and learning to identify high-risk states and treatments,” *Advances in Neural Information Processing Systems*, vol. 34, pp. 4856–4870, 2021.
- [4] S. Tang, M. Makar, M. Sjoding, F. Doshi-Velez, and J. Wiens, “Leveraging factored action spaces for efficient offline reinforcement learning in healthcare,” *Advances in Neural Information Processing Systems*, vol. 35, pp. 34 272–34 286, 2022.
- [5] F. Kamran, D. Tjandra, A. Heiler, *et al.*, “Evaluation of sepsis prediction models before onset of treatment,” *NEJM AI*, A10a2300032, 2024.
- [6] Z. Zhou, Z. Yang, S. Jiang, *et al.*, “Personalized virtual reality simulation training system for percutaneous needle insertion and comparison of zspace and vive,” *Computers in Biology and Medicine*, vol. 146, p. 105 585, 2022.
- [7] N. Prasad, L. F. Cheng, C. Chivers, M. Draugelis, and B. E. Engelhardt, “A reinforcement learning approach to weaning of mechanical ventilation in intensive care units,” in *33rd Conference on Uncertainty in Artificial Intelligence, UAI 2017*, 2017.
- [8] A. Raghu, M. Komorowski, L. A. Celi, P. Szolovits, and M. Ghassemi, “Continuous state-space models for optimal sepsis treatment: A deep reinforcement learning approach,” in *Machine Learning for Healthcare Conference*, PMLR, 2017, pp. 147–163.
- [9] A. Raghu, M. Komorowski, and S. Singh, “Model-based reinforcement learning for sepsis treatment,” *arXiv preprint arXiv:1811.09602*, 2018.
- [10] L.-F. Cheng, N. Prasad, and B. E. Engelhardt, “An optimal policy for patient laboratory tests in intensive care units,” in *BIOCOMPUTING 2019: Proceedings of the Pacific Symposium*, World Scientific, 2018, pp. 320–331.
- [11] M. Komorowski, L. A. Celi, O. Badawi, A. C. Gordon, and A. A. Faisal, “The artificial intelligence clinician learns optimal treatment strategies for sepsis in intensive care,” *Nature medicine*, vol. 24, no. 11, pp. 1716–1720, 2018.
- [12] R. Lin, M. D. Stanley, M. M. Ghassemi, and S. Nemati, “A Deep Deterministic Policy Gradient Approach to Medication Dosing and Surveillance in the ICU,” *2018 40th Annual International Conference of the IEEE Engineering in Medicine and Biology Society (EMBC)*, Jul. 2018. DOI: [10.1109/embc.2018.8513203](https://doi.org/10.1109/embc.2018.8513203). [Online]. Available: <http://dx.doi.org/10.1109/embc.2018.8513203>.
- [13] A. Peine, A. Hallawa, J. Bickenbach, *et al.*, “Development and validation of a reinforcement learning algorithm to dynamically optimize mechanical ventilation in critical care,” *npj Digital Medicine*, vol. 4, no. 1, Feb. 2021. DOI: [10.1038/s41746-021-00388-6](https://doi.org/10.1038/s41746-021-00388-6).
- [14] M. Mollura, C. Drudi, L.-W. Lehman, and R. Barbieri, “A reinforcement learning application for optimal fluid and vasopressor interventions in septic icu patients,” in *2022 44th Annual International Conference of the IEEE Engineering in Medicine & Biology Society (EMBC)*, IEEE, 2022, pp. 321–324.
- [15] X. Peng, Y. Ding, D. Wihl, *et al.*, “Improving Sepsis Treatment Strategies by Combining Deep and Kernel-Based Reinforcement Learning,” *American Medical Informatics Association Annual Symposium*, vol. 2018, pp. 887–896, Dec. 2018.

- [16] J. Liu, Y. Xie, X. Shu, *et al.*, “Value function assessment to different rl algorithms for heparin treatment policy of patients with sepsis in icu,” *Artificial Intelligence in Medicine*, vol. 147, p. 102726, 2024.
- [17] X. Wu, R. Li, Z. He, T. Yu, and C. Cheng, “A value-based deep reinforcement learning model with human expertise in optimal treatment of sepsis,” *npj Digital Medicine*, vol. 6, no. 1, p. 15, 2023.
- [18] C. Yu and Q. Huang, “Towards more efficient and robust evaluation of sepsis treatment with deep reinforcement learning,” *BMC Medical Informatics and Decision Making*, vol. 23, no. 1, p. 43, 2023.
- [19] G. Brockman, V. Cheung, L. Pettersson, *et al.*, *Openai gym*, 2016. eprint: [arXiv:1606.01540](https://arxiv.org/abs/1606.01540).
- [20] M. Oberst and D. Sontag, “Counterfactual off-policy evaluation with gumbel-max structural causal models,” in *International Conference on Machine Learning*, PMLR, 2019, pp. 4881–4890.
- [21] A. Kumar, A. Zhou, G. Tucker, and S. Levine, “Conservative q-learning for offline reinforcement learning,” *Advances in Neural Information Processing Systems*, vol. 33, pp. 1179–1191, 2020.
- [22] S. Fujimoto, E. Conti, M. Ghavamzadeh, and J. Pineau, “Benchmarking batch deep reinforcement learning algorithms,” *arXiv preprint arXiv:1910.01708*, 2019.
- [23] D. M. Roijers, P. Vamplew, S. Whiteson, and R. Dazeley, “A survey of multi-objective sequential decision-making,” *Journal of Artificial Intelligence Research*, vol. 48, pp. 67–113, 2013.
- [24] C. F. Hayes, R. Rădulescu, E. Bargiacchi, *et al.*, “A practical guide to multi-objective reinforcement learning and planning,” *Autonomous Agents and Multi-Agent Systems*, vol. 36, no. 1, p. 26, 2022.
- [25] S. Mannor and N. Shimkin, “The Steering Approach for Multi-Criteria Reinforcement Learning,” *Neural Information Processing Systems*, vol. 14, pp. 1563–1570, Jan. 2001.
- [26] G. Tesauro, R. Das, H. Chan, *et al.*, “Managing Power Consumption and Performance of Computing Systems Using Reinforcement Learning,” *Neural Information Processing Systems*, vol. 20, pp. 1497–1504, Dec. 2007.
- [27] S. Natarajan and P. Tadepalli, “Dynamic preferences in multi-criteria reinforcement learning,” en, in *Proceedings of the 22nd international conference on Machine learning - ICML '05*, Bonn, Germany: ACM Press, 2005, pp. 601–608, ISBN: 9781595931801. DOI: [10.1145/1102351.1102427](https://doi.org/10.1145/1102351.1102427). [Online]. Available: <http://portal.acm.org/citation.cfm?doid=1102351.1102427> (visited on 01/20/2023).
- [28] K. Van Moffaert, M. M. Drugan, and A. Nowe, “Scalarized multi-objective reinforcement learning: Novel design techniques,” *2013 IEEE Symposium on Adaptive Dynamic Programming and Reinforcement Learning (ADPRL)*, Apr. 2013. DOI: [10.1109/adprl.2013.6615007](https://doi.org/10.1109/adprl.2013.6615007). [Online]. Available: <http://dx.doi.org/10.1109/adprl.2013.6615007>.
- [29] H. Mossalam, Y. M. Assael, D. M. Roijers, and S. Whiteson, “Multi-Objective Deep Reinforcement Learning,” *arXiv: Artificial Intelligence*, Oct. 2016.
- [30] J. Xu, Y. Tian, P. Ma, D. Rus, S. Sueda, and W. Matusik, “Prediction-Guided Multi-Objective Reinforcement Learning for Continuous Robot Control,” *International Conference on Machine Learning*, vol. 1, pp. 10607–10616, Jul. 2020.
- [31] L. Barrett and S. Narayanan, “Learning all optimal policies with multiple criteria,” *Proceedings of the 25th international conference on Machine learning - ICML '08*, 2008. DOI: [10.1145/1390156.1390162](https://doi.org/10.1145/1390156.1390162). [Online]. Available: <http://dx.doi.org/10.1145/1390156.1390162>.
- [32] K. Hiraoka, M. Yoshida, and T. Mishima, “Parallel reinforcement learning for weighted multi-criteria model with adaptive margin,” *Cognitive Neurodynamics*, vol. 3, no. 1, pp. 17–24, Oct. 2008. DOI: [10.1007/s11571-008-9066-9](https://doi.org/10.1007/s11571-008-9066-9). [Online]. Available: <http://dx.doi.org/10.1007/s11571-008-9066-9>.
- [33] H. Iima and Y. Kuroe, “Multi-objective reinforcement learning for acquiring all Pareto optimal policies simultaneously - Method of determining scalarization weights,” *2014 IEEE International Conference on Systems, Man, and Cybernetics (SMC)*, Oct. 2014. DOI: [10.1109/smc.2014.6974022](https://doi.org/10.1109/smc.2014.6974022). [Online]. Available: <http://dx.doi.org/10.1109/smc.2014.6974022>.

- [34] D. J. Lizotte and E. B. Laber, “Multi-objective markov decision processes for data-driven decision support,” *The Journal of Machine Learning Research*, vol. 17, no. 1, pp. 7378–7405, 2016.
- [35] M. M. Fard and J. Pineau, “Non-deterministic policies in markovian decision processes,” *Journal of Artificial Intelligence Research*, vol. 40, pp. 1–24, 2011.
- [36] S. Tang, A. Modi, M. Sjoding, and J. Wiens, “Clinician-in-the-loop decision making: Reinforcement learning with near-optimal set-valued policies,” in *International Conference on Machine Learning*, PMLR, 2020, pp. 9387–9396.
- [37] S. Liu, K. C. See, K. Y. Ngiam, L. A. Celi, X. Sun, and M. Feng, “Reinforcement Learning for Clinical Decision Support in Critical Care: Comprehensive Review,” *Journal of Medical Internet Research*, vol. 22, no. 7, e18477, Jul. 2020. DOI: [10.2196/18477](https://doi.org/10.2196/18477). [Online]. Available: <http://dx.doi.org/10.2196/18477>.
- [38] J. Futoma, S. Hariharan, M. Sendak, *et al.*, “An Improved Multi-Output Gaussian Process RNN with Real-Time Validation for Early Sepsis Detection,” *arXiv: Machine Learning*, Aug. 2017. [Online]. Available: <https://arxiv.org/pdf/1708.05894.pdf>.
- [39] S. Saria, “Individualized sepsis treatment using reinforcement learning,” *Nature Medicine*, vol. 24, no. 11, pp. 1641–1642, Nov. 2018. DOI: [10.1038/s41591-018-0253-x](https://doi.org/10.1038/s41591-018-0253-x). [Online]. Available: <http://dx.doi.org/10.1038/s41591-018-0253-x>.
- [40] S. Tang, A. Modi, M. W. Sjoding, and J. Wiens, “Clinician-in-the-Loop Decision Making: Reinforcement Learning with Near-Optimal Set-Valued Policies,” *International Conference on Machine Learning*, vol. 1, pp. 9387–9396, Jul. 2020. [Online]. Available: <http://proceedings.mlr.press/v119/tang20c/tang20c.pdf>.
- [41] W. D. Miller, X. Han, M. E. Peek, D. C. Ashana, and W. F. Parker, “Accuracy of the sequential organ failure assessment score for in-hospital mortality by race and relevance to crisis standards of care,” *JAMA network open*, vol. 4, no. 6, e2113891–e2113891, 2021.
- [42] A. Irpan, K. Rao, K. Bousmalis, H. C. K, J. Ibarz, and S. Levine, “Off-Policy Evaluation via Off-Policy Classification,” *Neural Information Processing Systems*, vol. 32, pp. 5437–5448, Dec. 2018. [Online]. Available: <https://arxiv.org/pdf/1906.01624.pdf>.
- [43] M. Fatemi, S. Sharma, H. Van Seijen, and S. E. Kahou, “Dead-ends and Secure Exploration in Reinforcement Learning,” *International Conference on Machine Learning*, vol. 97, pp. 1873–1881, May 2019. [Online]. Available: <http://proceedings.mlr.press/v97/fatemi19a/fatemi19a.pdf>.
- [44] T. W. Killian, S. Parbhoo, and M. Ghassemi, “Risk sensitive dead-end identification in safety-critical offline reinforcement learning,” *Transactions on Machine Learning Research*, 2022.
- [45] H. Van Hasselt, A. Guez, and D. Silver, “Deep reinforcement learning with double q-learning,” in *Proceedings of the AAAI conference on artificial intelligence*, vol. 30, 2016.
- [46] Z. Song, R. Parr, and L. Carin, “Revisiting the softmax bellman operator: New benefits and new perspective,” in *International conference on machine learning*, PMLR, 2019, pp. 5916–5925.
- [47] J. -. Vincent, R. Moreno, J. Takala, *et al.*, “The SOFA (Sepsis-related Organ Failure Assessment) score to describe organ dysfunction/failure,” *Intensive Care Medicine*, vol. 22, no. 7, pp. 707–710, Jul. 1996, ISSN: 1432-1238. DOI: [10.1007/BF01709751](https://doi.org/10.1007/BF01709751). [Online]. Available: <https://doi.org/10.1007/BF01709751>.
- [48] A. E. Johnson, T. J. Pollard, L. Shen, *et al.*, “Mimic-iii, a freely accessible critical care database,” *Scientific data*, vol. 3, no. 1, pp. 1–9, 2016.
- [49] A. Elixhauser, C. Steiner, D. R. Harris, and R. M. Coffey, “Comorbidity measures for use with administrative data,” *Medical care*, pp. 8–27, 1998.
- [50] T. Mikolov, K. Chen, G. Corrado, and J. Dean, “Efficient estimation of word representations in vector space,” in *1st International Conference on Learning Representations, ICLR 2013, Scottsdale, Arizona, USA, May 2-4, 2013, Workshop Track Proceedings*, Y. Bengio and Y. LeCun, Eds., 2013. [Online]. Available: <http://arxiv.org/abs/1301.3781>.

- [51] S. Lambden, P. F. Laterre, M. M. Levy, and B. Francois, “The sofa score—development, utility and challenges of accurate assessment in clinical trials,” *Critical Care*, vol. 23, no. 1, pp. 1–9, 2019.
- [52] G. Gernardin, C. Pradier, F. Tiger, P. Deloffre, and M. Mattei, “Blood pressure and arterial lactate level are early indicators of short-term survival in human septic shock,” *Intensive care medicine*, vol. 22, pp. 17–25, 1996.
- [53] S. Tang and J. Wiens, “Model selection for offline reinforcement learning: Practical considerations for healthcare settings,” in *Machine Learning for Healthcare Conference*, PMLR, 2021, pp. 2–35.
- [54] O. Gottesman, F. Johansson, J. Meier, *et al.*, “Evaluating reinforcement learning algorithms in observational health settings,” *arXiv preprint arXiv:1805.12298*, 2018.

A Different Biomarkers Along Patient Trajectory

To demonstrate the advantages and limitations of the intermediate reward signals, Figure 5 presents the survival, SOFA score, and arterial lactate data gathered across a specific patient trajectory. The SOFA score and arterial lactate values offer a detailed view of the patient's health progression. However, they are not perfectly correlated with mortality; thus, optimizing these parameters alone may not suffice for learning the optimal policy.

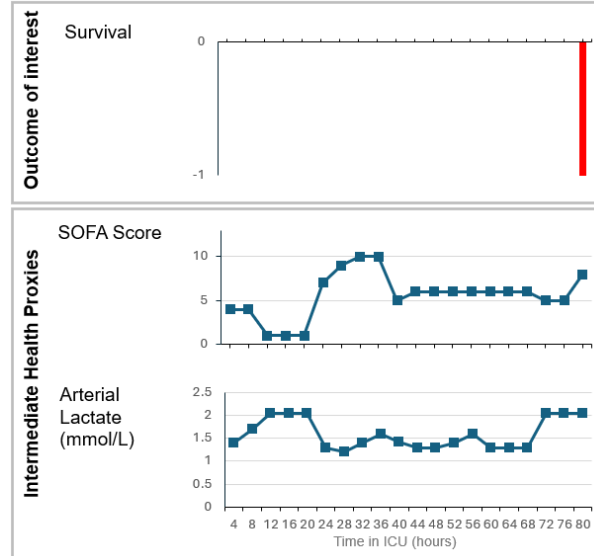


Figure 5: Intermediate and sparse reward signals along the patient trajectory.

B Pruned Q-Learning Under Different Noise Levels

We analyze how Pruned QL behaves as the intermediate reward signal becomes less precise. To achieve this we conduct an experiment where we add white noise with standard deviations of 0.1, 1, and 10 to the intermediate rewards. Figure 6 depicts the results. We observe that Pruned QL remains robust until raising the white noise standard deviation to 10, where it only does marginally better than the baseline. This result illustrates two important characteristics of our method. First, it shows that Pruned QL has generally high robustness to noise. Second, the fact that the performance drops when the noise standard deviation is increased to 10 indicates that the intermediate rewards considered in this method must carry some relevant information about the sparse outcome of interest. At a white noise standard deviation of 10, the signal-to-noise ratio (SNR) of the shape reward is less than 0.5 and the SNR for the fuel rewards is less than 0.02, diluting nearly the entirety of the reward signal. This result is robust for various pruning strengths.

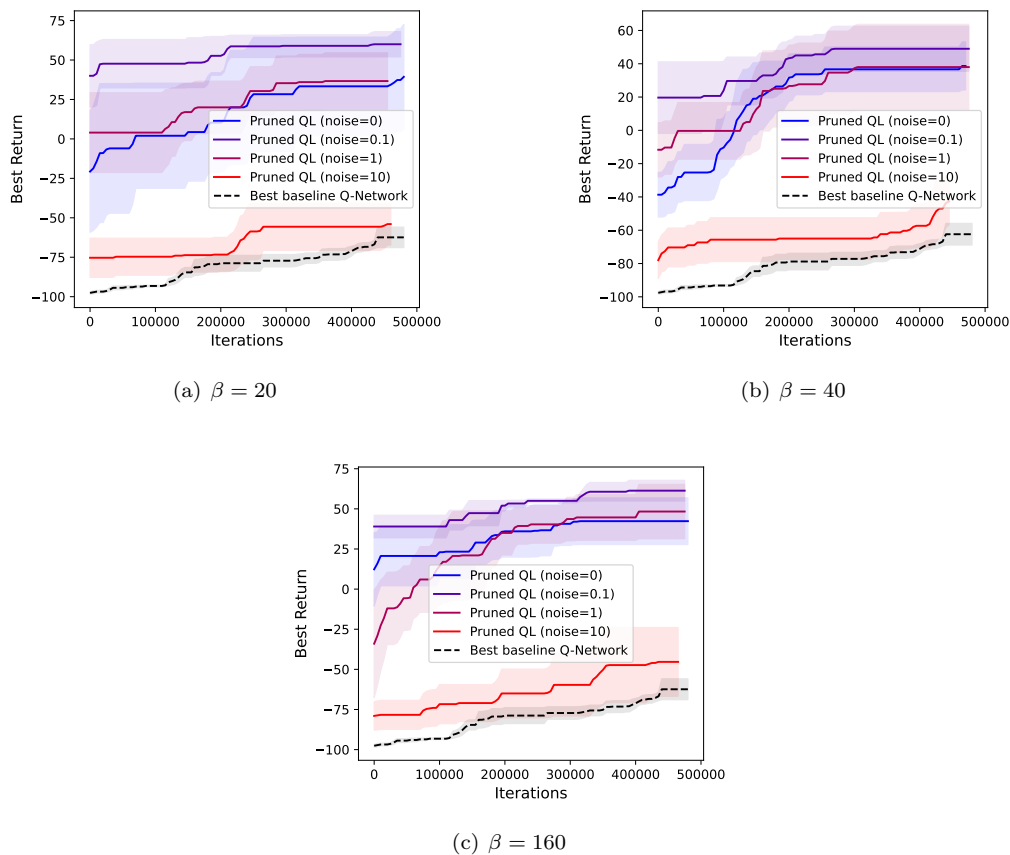


Figure 6: Learning curves indicating policy performance of Pruned QL vs. best baseline Q-Network under different noise levels.

C Further Insights From MIMIC-III Experiments

C.1 Survival Rate by Q-value for different pruning strengths

To further analyze the Q-values obtained from Pruned CQL, we calculated the mean Q-values for each patient trajectory in the test data and divided them into 100 percentile bins. For each bin, we determined the probability of patient survival. Figure 7 presents the survival rate per bin for Pruned CQL with a conservativity level of $\alpha = 0.001$ and varying pruning strictness. The analysis demonstrates a strong positive relationship across different pruning strengths. For instance, with a pruning strength of 40, we observe a survival rate below 30% for state-action pairs with the lowest Q-values and over 80% for those with the highest Q-values. These results indicate that the Pruned CQL policies are based on Q-functions that effectively distinguish between high- and low-risk state-action pairs, which is crucial for identifying relevant policies.

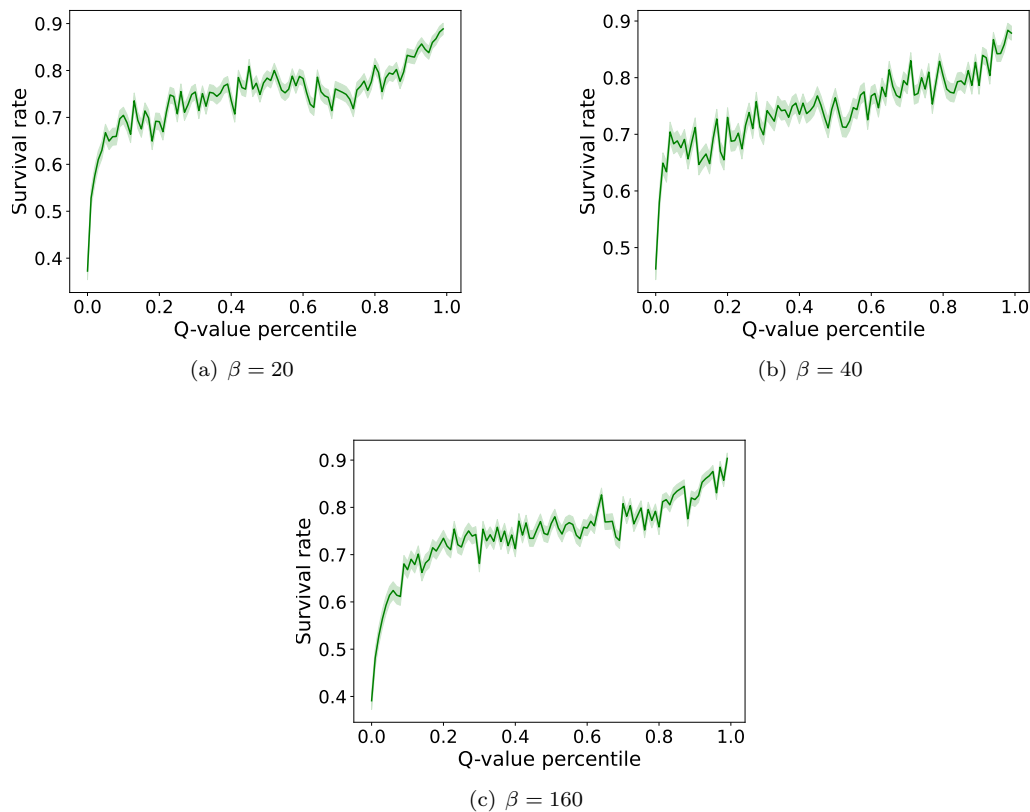
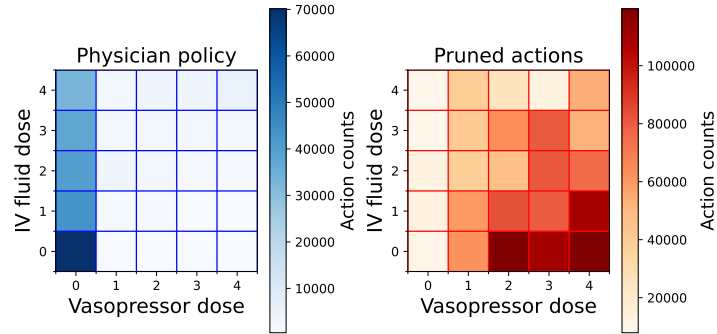


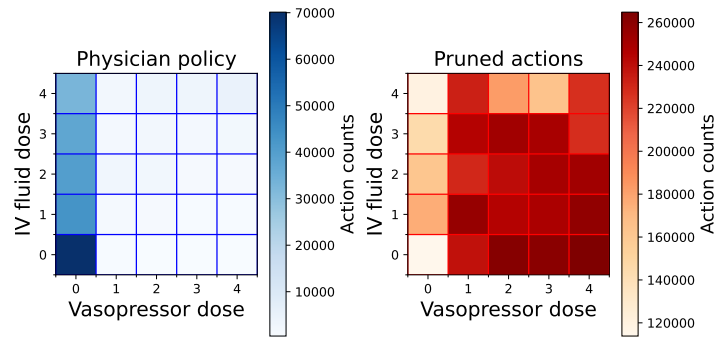
Figure 7: Survival rate by Pruned CQL Q-value percentile plotted for 100 equal-sized bins and different pruning strength.

C.2 Pruned Action Distribution for Different Pruning Strengths

To augment the findings illustrated in Figure 4, we depict the distribution of removed actions for the pruning strength values $\beta = 20, 160$ in Figure 8.



(a) $\beta = 20$



(b) $\beta = 160$

Figure 8: Distribution of pruned actions for different pruning strengths.